Engineering and Technology Journal
Journal homepage: https://etj.uotechnology.edu.iq

Experimental and Multi-Optimization Investigation of Machining (X210) Alloy Steel Using Angled EDM Electrodes

Ahmed M. Abbas[a,b*], **Ali Abbar Khleif** [b]

[a,b] Mechanical Engineering Dept., Hawija Institute, Northern Technical University, Kirkuk, Iraq.
[b] Production Engineering and Metallurgy Dept., University of Technology-Iraq, Alsina'a street, 10066 Baghdad, Iraq.
*Corresponding author Email:ahmedabas_hwj@ntu.edu.iq

HIGHLIGHTS

- A new electrode design with horizontal flushing hole
- The novel design improves Hardness and reduce surface roughness of Alloy Steel (X210).
- A 3D contour diagrams are achieved to determine the importance of each parameter.
- A good agreement between standard deviation and coefficient of variation for predicted and actuals values.
- A 45º angled electrode has the lowest value of surface roughness.

ARTICLE INFO

Handling editor: Omar Hassoon

Keywords:
EDM, Electrode Geometry, Roughness, Hardness, DOE.

ABSTRACT

Electrical Discharging Machining (EDM) offers broad capabilities that allow it to be used in the manufacturing, automotive, and aviation industries, as well as practically all disciplines of conductive material machining. This experimental and numerical work aims to use EDM to evaluate the surface of Alloy Steel (X210). The experiments used the EDM copper electrode with a novel horizontal flushing hole. The findings of the investigations have been analyzed so that the best settings for the input process factors can be determined. Alloy tool steel (X210) is cut in dimensions by the Wire EDM (dk7740) (15 × 15 × 10 mm) with very little research dealing with this alloy. ARL spectrometer method was used to determine the percentage chemical composition. In the current experimental work, the Effect of different parameters such as electrode angle (EA), peak current (Ip), pulse on time (Pon), and pulse off time (Poff) have been investigated using response surface methodology (RSM). Microhardness reaches the maximum value with an electrode angle of 67.5º with increasing current and pulse. Responses (SR and MH) were modeled using RSM. It is found that the lowest SR is achieved when conducted with an electrode tilt of 45º. A high peak current (Ip) has also been discovered to raise SR further while decreasing pulse-off time. The primary effects of input parameters, specifically E.A, Ip, Pon, and Poff, were determined to impact the Ra and MH considerably. Peak current greatly affects 45º angled electrodes while keeping other parameters constant.

1. Introduction

Electrical Discharge Machining (EDM) is a commonly employed technique for machining difficult-to-machine metals. This process involves the removal of material from the workpiece by subjecting it to a series of electric sparks, which result in localized melting. The work material has been subjected to removal by the spark, resulting in the erosion of a small portion of the electrode tool substance. Machining complicated and hard materials with conventional methods could be inconvenient and time-wasting. Furthermore, the surface quality of the finished parts with traditional methods is low [1, 2]. Electrical Discharge Machining EDM acts on the rule of metal erosion by energy as a thermoelectric between the workpiece and the electrode tool. Due to the complex shape of the tool used to cut, it is possible to replace it with a conductive electrode and regulate the electrode's movements along related axes. EDM avoids the challenges encountered in conventional machining [3, 4]. The manufacturing industry faces a challenge whenever it must create slots or holes in hard substances while maintaining a high degree of geometrical accuracy. The existence of undercuts in EDM is one of the most important issues [5], which eventually affects the geometrical precision. It has been stated that the undercut, particularly in the case of die production by EDM [6, 7], is extremely difficult to predict due to a complicated and non-linear relationship between tool wear, tool diameter, and process parameters. This can be particularly relevant when the undercut arises from tool wear [8, 9].

Ahsan Khan et al. [10] investigated the effect of electrode shape on some of the variables for carbon steel with electrode copper material. The electrode geometries were square, diamond, triangle, and round. The round electrode was the best in

http://doi.org/10.30684/etj.2023.143826.1612
Received 14 October 2023; Received in revised form 21 November 2023; Accepted 10 December 2023; Available online 03 January 2024
2412-0758/University of Technology-Iraq, Baghdad, Iraq

MRR, followed by other shapes. Diamond electrode approved better MRR and EWR. Jitendra et al. [11] investigated a new tool design to enhance the performance of EDM. Zircaloy_2 is used along the Cu electrode with varying angles of rake by (0°, 45°, and 60°), different values in flat land (2 mm), and different relief angles. By increasing the rake angle, MRR is increased.

Nadeem et al. [12] reported using a conventional tool with relief angles added to the tool electrodes. WC and copper were the workpiece and electrode. Using relief-angled electrodes has resulted in a 49% reduction in the machining time. N. Pellicer et al. [13] Different electrode geometry is investigated in this paper. Rectangle and square geometry show high accuracy in groove processing due to the high EWR and machining stability. The triangular electrode is inefficient because the edges of the triangular shape wear speedy.

Rahul Davis et al. [14] Hollow and solid copper electrodes have been fabricated in this study for holes drilling in composites of quenched tool copper with high hardness. MRR is raised with increasing duty factor and current for two types of electrodes. Conical electrodes had a lesser roughness comprised of hollow electrodes. Hollow electrodes show an increase in tool wear compared to solid. Smrutirekha and Masanta [15] studied an experiment on hexagonal electrodes. Al alloy (A6063) plate was a workpiece. The increasing high current and spark power induced greater crater and improved MRR. Mahesh and Tajane [16] concluded that the best machining achievement is gained when the workpiece is the anode and the electrode is the cathode. The geometry of the electrode with a circular shape gives a high MRR and less tool wear percentage. Round shapes produce surfaces that are smoother and then square.

Junjie Li et al. [17] performed an electrode tool path simulated method to test all faces of molds to study all the uncut zones precisely that cannot be checked and performed by the other cutters. The efficiency of this EDM tool could be enhanced by 70%. Kamlesh et al. [18] presented a study on the effect of electrode geometry on surface quality and MRR. The electrode shape is the most impact factor that influences the functional measures. The Contribution rate of electrode shape is approximately (10-20)% for ANOVA and S/N ratio, and the quality of surface and MRR is enhanced at these values. Bhola Jha and Mohan Rao [19] reported on an EDM review of the papers on electrode tool design and manufacturing to optimize and minimize production time. Electrode Design and manufacturing had an essential role in EDM evolution in the future. There have been no reports of angled electrode work utilizing EDM Alloy steel (X210) as the working material. A limited amount of work is available on the multi-response optimization of the electrical discharge machining (EDM) process when using an angled electrode with a transverse hole electrode.

2. Novelty of The Study

There are numerous contribution to this work, as follow:

1) New angled electrode (22.5° and 67.5°).
2) Vertical flushing hole has been replaced with one having a side flushing hole.
3) The workpiece is Alloy steel (X210).

3. Materials and Methods

Alloy tool steel (X210) is cut in dimensions by the Wire EDM (dk7740) (15 × 15 × 10 mm). The ARL spectrometer method was used to determine the percentage chemical composition (wt.%), given in Table 1.

According to the literature survey, no more studies selected those parameters besides the different angles of electrodes. Table 2 lists the values for the various process factors and variables. This study aimed to modify the standard cylindrical design by including several design types, notably by introducing electrodes angled on the sides of the tool. Figure 1 shows the geometry of electrodes with their angles.

Table 1: Chemical elements composition Alloy steel X210

Elements	C	Cr	Mn	Cu	Zn	Mo	Sn	Fe
% wt.	1.9	11.71	0.49	0.36	0.15	0.24	2.22	Remainder

Table 2: Interesting factors and their levels

Factors	Parameters	Levels				
		1	2	3	4	5
A	Electrode angle (deg)	0	22.5º	45 º	67.5 º	90 º
B	Peak current(Amp)	15	20	25	30	35
C	Pulse on time (µs)	75	150	225	300	375
D	Pulse of time (µs)	20	50	80	110	140

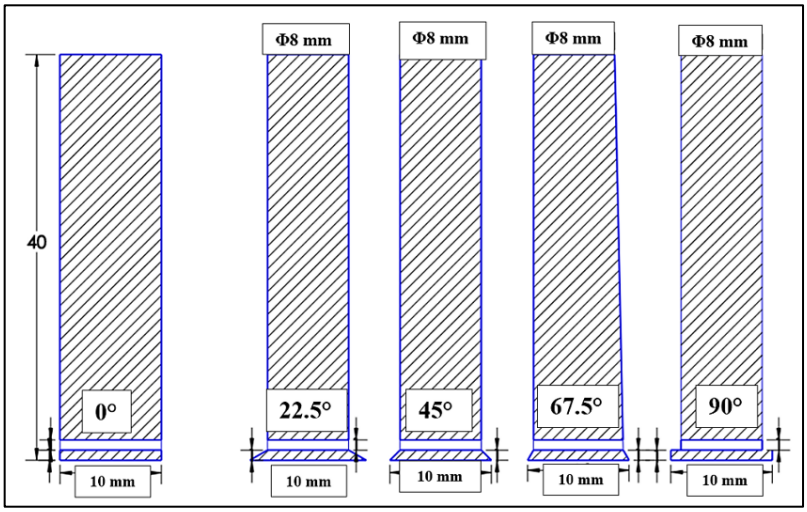

Figure 1: Electrode types with different angles

The tool was made of Cu and achieved in a 10 mm diameter rod of sparking area with 400 mm length and a transverse hole for flushing [20]. A die sink EDM machine (CM 323-50N (CHAMBER) was used to generate a 10 mm hole on the surface of specimens. Based on initial experiments, a Schematic sketch of the progressive electrode design and machined surface is shown in Figure 2.

In hypothesis tests, the effective use of the P-value is evaluated to determine whether or not to reject a null hypothesis. The null hypothesis is assumed to be correct. In statistics, the p-value indicates significance, which is the probability of receiving a result at least as extreme as the one obtained. In many contexts, a p-value of 0.05 is considered significant [21].

The analysis of variance (ANOVA) method is utilized to illustrate the different sources of variation, the degree of freedom (DF), adjusted mean square error (Adj MS), adjusted sum square error (Adj SS), sequential sum square error (Seq SS), Fisher's statistical test (F-test), and the corresponding probability values (p-values) in the columns [22].

Experiments are designed to measure the influence of electrode angle geometry on response measures. All other parameters, such as Voltage value, Polarity, and dielectric type, were considered constant, as shown in Table 3. Actual images of the Cu tool are shown in Figure 3, and detailed descriptions of the tools are given in Table 4. Response parameters (SR and MH) are analyzed after EDM machining.

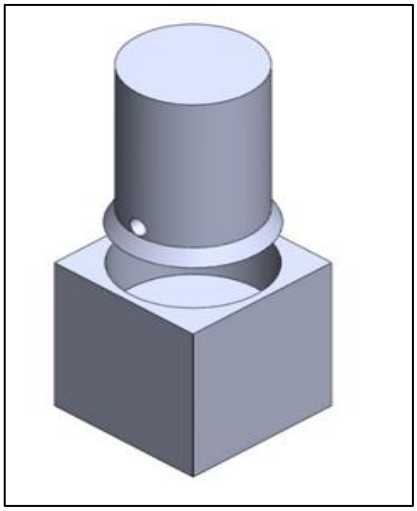

Figure 2: The geometry of the angled electrode and workpiece

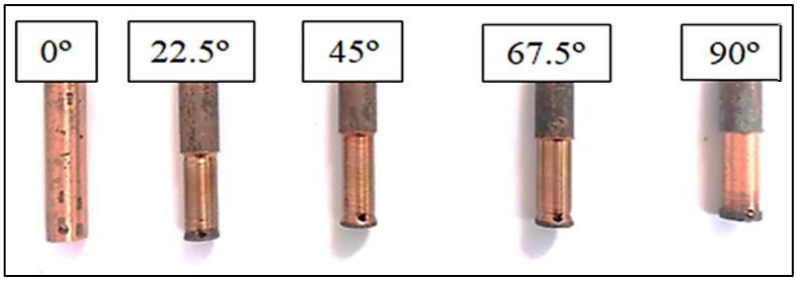

Figure 3: Electrodes with different angles produced by (DK7740) WEDM

Table 3: Constant parameters

No	Machining settings	Constant
1	Voltage value	240 Volt
2	Polarity	Direct
3	Type of dielectric	kerosene

Table 4: Experiment design

No	Electrode Angle (deg)	Ip (Amp)	Pon (µs)	Poff (µs)
1	22.5	20	150	50
2	67.5	20	150	50
3	22.5	30	150	50
4	67.5	30	150	50
5	22.5	20	375	50
6	67.5	20	375	50
7	22.5	30	375	50
8	67.5	30	375	50
9	22.5	20	150	110
10	67.5	20	150	110
11	22.5	30	150	110
12	67.5	30	150	110
13	22.5	20	375	110
14	67.5	20	375	110
15	22.5	30	375	110
16	60	30	375	110
17	0	25	225	80
18	90	25	225	80
19	45	15	225	80
20	45	35	225	80
21	45	25	75	80
22	45	25	300	80
23	45	25	225	20
24	45	25	225	140
25	45	25	225	80
26	45	25	225	80
27	45	25	225	80
28	45	25	225	80
29	45	25	225	80
30	45	25	225	80

The surface roughness was measured with a portable stylus-type Profile-meter, designed explicitly to measure surface roughness (SR), as shown in Figure 4. Hardness Tester THL306 roll special-purpose hardness tester is a professional measuring roll hardness tester. The Hardness Tester is located at Northern Technical University Labs.

Different electrode angles have been machined by a wire electric discharging machine (DK7740). This machine is widely used in mold, bulk production, electronic equipment, precision machinery, medical equipment, auto parts, aerospace and military industries, etc. Figure 5 shows an image of 30 specimens for DOE analysis in alloy steel. Different electrode angles have been machined by a wire electric discharging machine (DK7740). This machine is widely used in mold, bulk production, electronic equipment, precision machinery, medical equipment, auto parts, aerospace and military industries, etc. Figure 5 shows an image of 30 specimens for DOE analysis in alloy steel.

Figure 4: Profile-meter for measuring (SR)

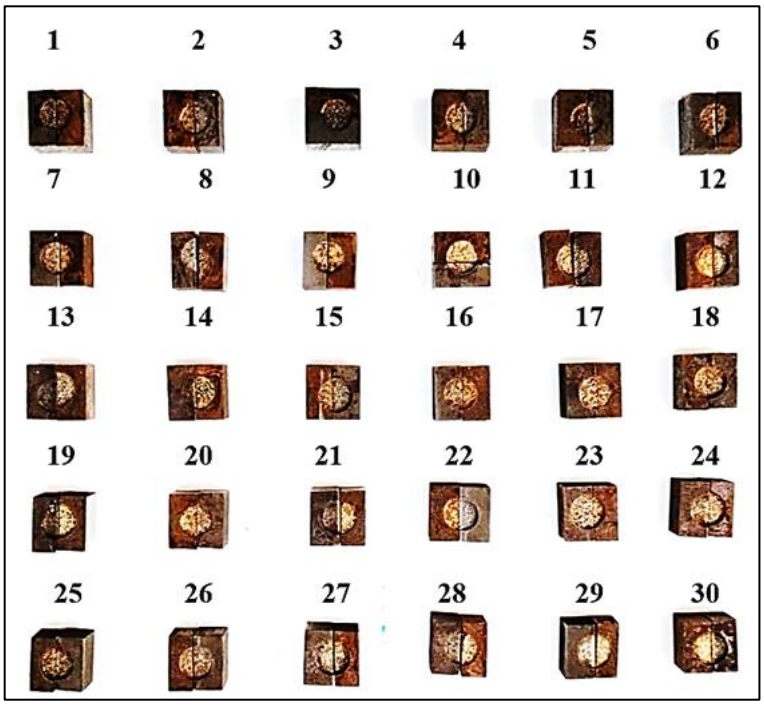

Figure 5: Workpiece Alloy steel (X210) after machining for L30 array

4. Results and Discussions

4.1 Surface Roughness Analysis

This experimental study focuses on the level of accuracy employed in achieving optimal surface quality throughout the surface alteration process of Alloy tool steel X210 through Electrical Discharge Machining (EDM). The trails are precisely planned and executed via response surface methodology. Design Expert 12 (DX 12) is utilized as the statistical program to generate the surface roughness (SR) regression model. The sum of squares, the lack of fit test, and mathematical model brief statistics were used to assess the constructed model's level of accuracy. An analysis of variance, often known as an ANOVA, is fulfilled to determine the importance of each parameter to keep SR at a minimum. To examine the effect that process variables have on SR, 3D contour diagrams are drawn. The results of the experiments on the surface roughness values are presented in Table 5.

The finding of the analysis of variance (ANOVA) for the constructed SR mathematical model is presented in Table 6. The F-value calculated for the expected SR model is 58.21, which implies that the model is statistically significant. The possibility of a higher F-value due to noise is only possible with a probability of 0.01%. In this case, (E-Angle) B(Current) C(Pulse-on) D(Pulse-off), BC, A^2, B^2, C^2, and Dare discovered significant phrases (P-value less than 0.05). With an F-value of 1.36, "lack of fit" is statistically really significant compared to pure error.

The 0.9044 R^2 predicted and the 0.9560 R^2 adjusted agree with one another within a relatively small range (smaller than 0.2). The signal-to-noise term is calculated by using Adeq Precision. It's favored to achieve a ratio larger than 4. In this scenario, the signal intensity at 28.6435 is sufficient. A regression model for surface roughness (SR) is created using regression analysis. A statistically significant impact (P-value larger than 0.05) is not considered throughout the regression analysis. Equation 1 shows the SR regression mathematical model.

$$\begin{aligned}\text{Regression mathematical model of SR} \;=\; & -0.312259 + 0.00659375 * \text{E} - \text{angle} + \\ & 0.111022 * \text{Current} + 0.000926126 * \text{Pulse} - \text{on} + 0.0104033 * \text{Pulse} - \text{off} + \\ & 0.000188351 * \text{E} - \text{angle} * \text{Current} - 3.31585\text{e} - 05 * \text{E} - \text{angle} * \text{Pulse} - \text{off} + \\ & 6.0816\text{e} - 05 * \text{Current} * \text{Pulse} - \text{on} - 7.97104\text{e} - 05 * \text{E} - \text{angle\^{}2} + -0.00188562 * \\ & \text{Current\^{}2} + -3.74813\text{e} - 06 * \text{Pulse} - \text{on\^{}2} + -4.98928\text{e} - 05 * \text{Pulse} - \text{off\^{}2} \qquad (1)\end{aligned}$$

Figure 6 and Figure 7 illustrate the graphical representation of the relationship between normal probability, externally studentized residuals, and the actual versus predicted SR individually. The plot results suggest a linear relationship between the actual SR and expected SR data, indicating a strong concordance between the predicted and actual values of SR. Therefore, the proposed SR model is very important. These findings were generally consistent with the earlier research [23].

Table 5: SR values and experiment matrix

Run	E-Angle. (deg)	Current. (Amp)	Pulse-on. (µs)	Pulse-off. (µs)	SR actual (µ/m)	SR predicted (µ/m)	Act/pred
1	45	25	375	80	5.927	5.657	1.048
2	45	25	225	80	5.792	5.477	1.058
3	22.5	20	300	110	4.349	4.412	0.986
4	45	25	225	80	5.778	5.477	1.055
5	45	25	225	140	5.203	5.635	0.923
6	67.5	20	150	50	3.982	4.055	0.982
7	22.5	20	150	50	3.511	3.850	0.912
8	45	35	225	80	6.819	6.498	1.049
9	90	25	225	80	5.416	5.215	1.039
10	22.5	30	300	110	6.112	6.198	0.986
11	45	25	225	20	5.237	5.407	0.969
12	45	25	225	80	5.903	5.477	1.078
13	45	15	225	80	3.441	3.137	1.097
14	67.5	30	150	50	5.532	5.773	0.958
15	0	25	225	80	5.214	4.757	1.096
16	67.5	20	300	110	4.265	4.631	0.921
17	45	25	75	80	5.019	4.624	1.085
18	67.5	30	300	50	6.599	6.333	1.042
19	22.5	30	150	110	5.572	5.643	0.987
20	45	25	225	80	5.714	5.477	1.043
21	22.5	20	150	110	4.111	3.946	1.042
22	22.5	30	150	50	4.844	5.528	0.876
23	67.5	20	300	50	4.151	4.527	0.917
24	67.5	20	150	110	4.083	4.153	0.983
25	45	25	225	80	5.600	5.477	1.022
26	22.5	30	300	50	5.753	6.077	0.947
27	67.5	30	150	110	5.758	5.890	0.978
28	22.5	20	300	50	4.150	4.311	0.963
29	67.5	30	300	110	6.480	6.456	1.004
30	45	25	225	80	5.386	5.477	0.983
						Mean	1.001
						Std. Dev.	0.051
						C.V	0.059

Table 6: ANOVA for SR

Source	Sum of Squares	Df	Mean Square	F-value	p-value	
Model	1.18	11	0.1074	58.21	< 0.0001	significant
A-E-angle	0.0265	1	0.0265	14.35	0.0013	
B-Current	0.9080	1	0.9080	49.27	< 0.0001	
C-Pulse-on	0.0779	1	0.0779	42.26	< 0.0001	
D-Pulse-off	0.0186	1	0.0186	10.09	0.0052	
AB	0.0072	1	0.0072	3.89	0.0640	
AD	0.0080	1	0.0080	4.35	0.0516	
BC	0.0083	1	0.0083	4.51	0.0478	
A^2	0.0447	1	0.0447	24.22	0.0001	
B^2	0.0610	1	0.0610	33.05	< 0.0001	
C^2	0.0122	1	0.0122	6.61	0.0192	
D^2	0.0553	1	0.0553	29.98	< 0.0001	
Residual	0.0332	18	0.0018			
Lack of Fit	0.0259	13	0.0020	1.36	0.3884	not significant
Pure Error	0.0073	5	0.0015			
Cor Total	1.21	29				
Std. Dev.	0.0429					
Mean	2.26					
C.V. %	1.90					
R^2	0.9727					
Adjusted R^2	0.9560					
Predicted R^2	0.9044					
Adeq Precision	28.6435					

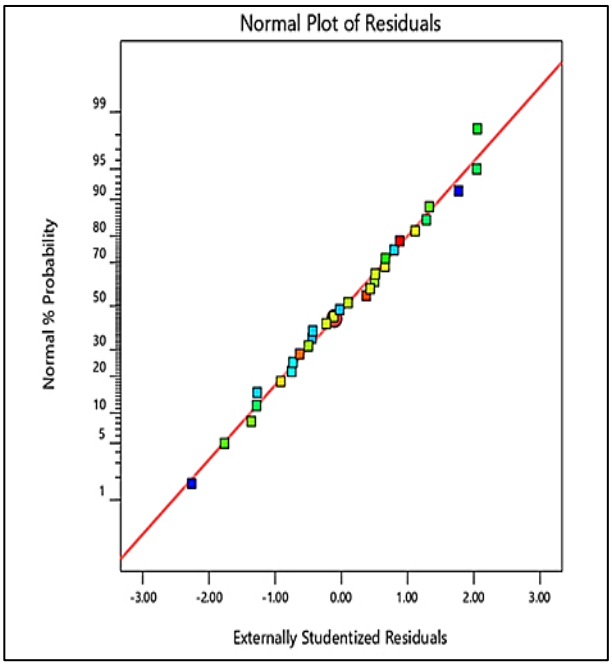

Figure 6: Normal vs. external studentized residuals

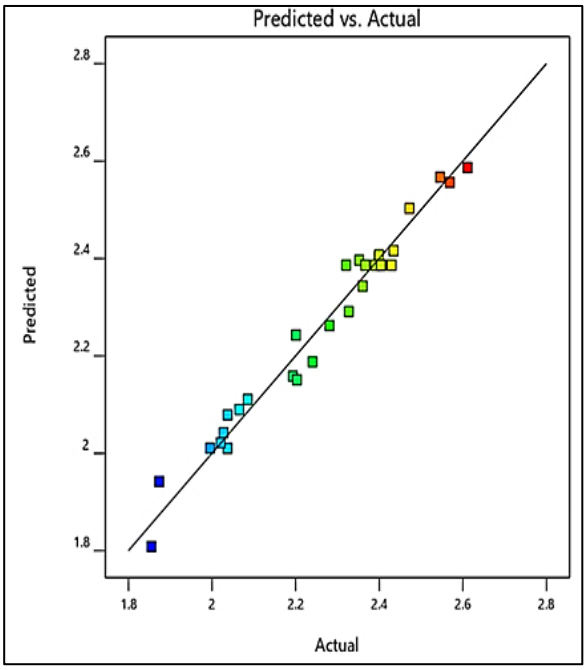

Figure 7: Predicted vs. Actual Surface roughness

Figure 8a is a 3D contour diagram of an RSM model illustrating the impacts of electrode angle at 45o with peak current and pulse on time on SR while maintaining a level of default Poff = 80µs is constant. It has been noticed that the maximum SR value varies with the peak current, and it was determined that the maximum SR value steadily increases for a specific rise in peak current and pulse. The high energy from discharging in the sparking area makes it easier to melt and dissipate material, so the SR increases with peak current at a 45° electrode angle. The effects of electrode angle 22.5º on min SR with a pulse on and current while keeping the default Poff = 50 µs fixed can be seen as a three-dimensional Contour diagram in Figure 8b. The effect of electrode angle at 45º on pulse off (µm) current on max SR while keeping the Pon = 225 µs constant is illustrated in Figure 8c. The variance of max SR has been noticed.

The results indicate a rise in current with moderate pulse off. There is a prolonged rise in SR. This increase in surface roughness is due to the accumulation of sparks at the ends of electrodes. In this situation, the more durable heat energy in the machining area degrades the surface's features. Furthermore, the effect of the electrode angle fixed at 22.5º, along with the pulse of time (Poff) and peak current (Ip), on the minimum (SR), is illustrated in Figure 8d as a three-dimensional Contour diagram. This analysis keeps a constant pulse at a level of 150 µm. These results coincide with some research [12, 15]

The relationship between surface roughness (SR) and pulse-off time and peak current has been investigated, leading to the idea that as the pulse-off time increases and the current decreases, there is a gradual decrease in surface roughness, eventually achieving a minimum value. The reduction in surface roughness observed at an angle of 22.5º can be explained by the reduced availability of heat over a shorter duration. Therefore, a minimum in SR was noticed during the machining process. The effect of electrode angle at 45º with pulse off (µs) and pulse on (µs) on max SR at maintaining the level of peak current constant is illustrated in Figure 9a. The variance of max has been determined, and it is found that there is a continual acceleration in surface roughness for raising the pulse to maximum value with a high value of current at 45º electrode angle.

A high peak current (Ip) has also been discovered to raise SR further while simultaneously decreasing pulse-off time. Similarly, the influence of electrode angle at 22.5º with pulse off (Poff) and pulse on time (Pon) on min SR, while maintaining the level of Ip = 25 amperes maintain constant is illustrated in Figure 9b as a three-dimensional Contour diagram. It has been determined that for an increase in pulse off, there is a continual drop in SR based on the observed variations of pulse on at minimum value with electrode angle 22.5º. Additionally, a further reduction in stress response (SR) might be noticed along with a rise in pulse on time. (Pon) while keeping current at minimum value. The results presented were compatible with earlier research [2].

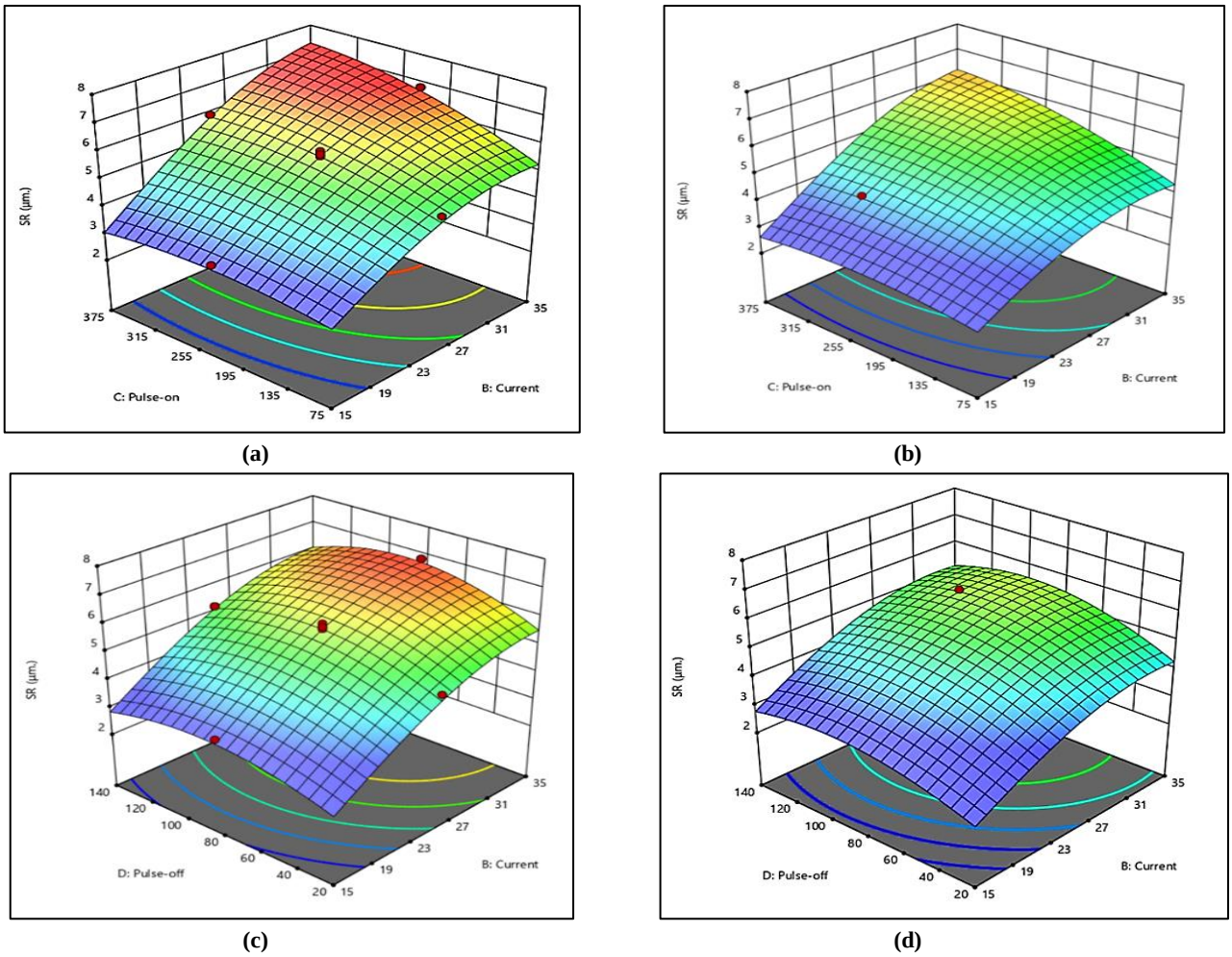

Figure 8: (a) Max SR vs. P_{on} and Current, (b) Min SR vs. P_{on} and current, (c) Max SR vs. P_{off} and current, (d) Min SR vs. P_{off} and Current

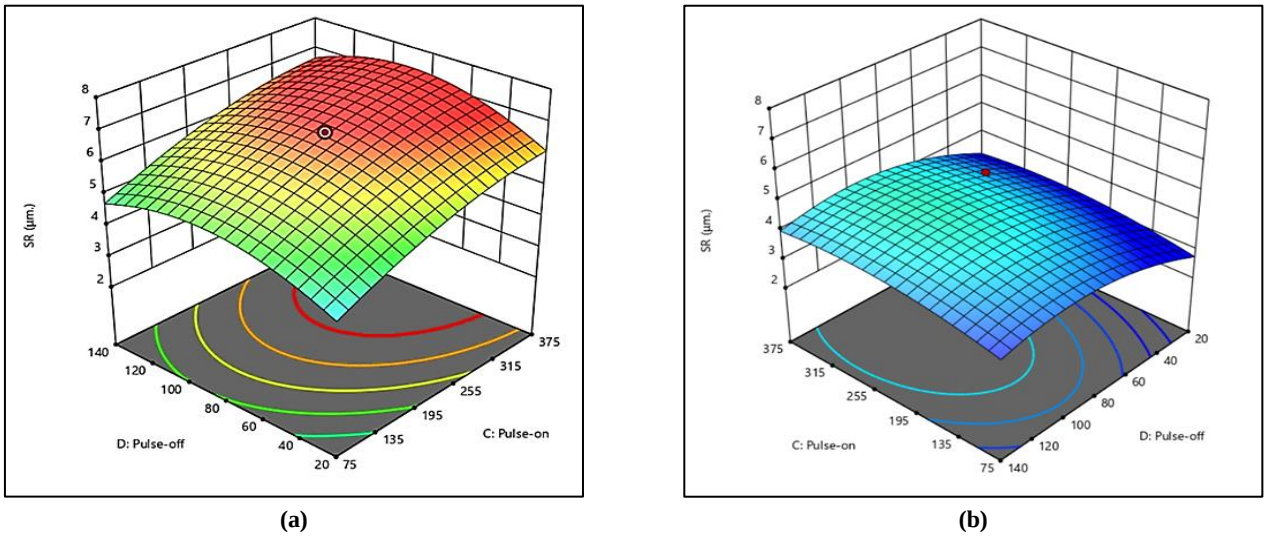

Figure 9: (a)Max SR vs. P_{off} and $P_{on,}$ (b) Min SR vs. P_{on} and P_o

4.2 Miro-Hardness (MH) Analysis

This experimental study aims to achieve optimal work surface microhardness by modifying the surface of Alloy tool steel (X210) employing electrical discharge machining (EDM). Experiments have been adequately designed and executed, applying response surface methodology. Three microhardness readings were obtained from distinct sites, and the average was selected as the ultimate microhardness value.

Hardness Tester The THL306 roll special-purpose hardness tester, as shown in Figure 10, is a professional measuring roll hardness tester as Table 7 described. The experimental procedure involved modifying many factors.

Figure 10: Hardness Tester THL306

Table 7: MH value and experimental matrix

Run	E-Angle (deg)	Current (Amp)	Pulse-on (µs)	Pulse-off (µs)	MH actual (VHN)	MH predicted (VHN)	Actu/Pred
1	45	25	375	80	530	541.343	1.021
2	45	25	225	80	504	480.545	0.953
3	22.5	20	300	110	410	395.747	0.965
4	45	25	225	80	465	480.545	1.033
5	45	25	225	140	505	529.872	1.049
6	67.5	20	150	50	412	395.611	0.960
7	22.5	20	150	50	355	353.254	0.995
8	45	35	225	80	620	619.557	0.999
9	90	25	225	80	480	434.171	0.905
10	22.5	30	300	110	611	586.011	0.959
11	45	25	225	20	512	433.627	0.847
12	45	25	225	80	410	480.545	1.172
13	45	15	225	80	360	359.170	0.998
14	67.5	30	150	50	490	462.887	0.945
15	0	25	225	80	590	347.707	0.589
16	67.5	20	300	110	420	440.509	1.049
17	45	25	75	80	514	423.367	0.824
18	67.5	30	300	50	533	585.881	1.099
19	22.5	30	150	110	530	463.003	0.874
20	45	25	225	80	520	480.545	0.924
21	22.5	20	150	110	470	395.718	0.842
22	22.5	30	150	50	420	416.971	0.993
23	67.5	20	300	50	390	395.640	1.014
24	67.5	20	150	110	400	440.479	1.101
25	45	25	225	80	487	480.545	0.987
26	22.5	30	300	50	520	534.075	1.027
27	67.5	30	150	110	470	511.322	1.088
28	22.5	20	300	50	380	353.281	0.930
29	67.5	30	300	110	660	640.222	0.970
30	45	25	225	80	435	480.545	1.105
						Mean	0.9739
						Std. Dev.	0.1099
						C.V	0.1128

The final result is the average of three microhardness measurements used for further investigation. The microhardness (MH) regression model is created with the statistical program Design Expert 12 (DX 12). The sum of squares, lack of fit test, and model data summary are used to assess the adequacy of the constructed model. ANOVA has also been used to determine the influence of each parameter on maximizing MH. Three-dimensional Contour diagrams are created to investigate the effect of factors on microhardness (MH). Table 7 shows the mean values of the results of the microhardness measurements.

The utilization of analysis of variance assesses the adequacy of the developed model. The finding of the analysis of variance (ANOVA) for the created (MH) design is presented in Table 8. The F-value calculated for the expected MH model is 14.79, suggesting that the mathematical model is statistically significant. A greater F-value due to noise is only possible in 0.01% of cases. In this particular case, the parameters A (E-Angle), B (Current), C (Pulse-on), D (Pulse-off), BC, and A2 have

been identified as significant statistically (with a p-value smaller than 0.05). The F-value for the "lack of fit" is 1.15, suggesting that the lack of fit is statistically important compared to the pure error.

The Predicted R^2 of 0.5244 is in reasoned acceptance with the Adjusted R^2 of 0.7404; i.e., the difference is less than 0.2. Adeq Precision measures the S/N ratio. A ratio larger than 4 is useful. In this case, 13.3878 indicates an adequate signal. Regression analysis is employed to construct a Microhardness (MH) regression model. In regression analysis, variables with non-significant P-values (higher than 0.05) are typically excluded from consideration. The mathematical regression model of MH is shown in Equation 2.

$$\text{Regression mathematical model of MH} = 17.8268 + 0.121198 * \text{E} - \text{angle} + -0.106462 * \text{Current} + -0.0358546 * \text{Pulse} - \text{on} + 0.0182936 * \text{Pulse} - \text{off} + 0.00179297 * \text{Current} * \text{Pulse} - \text{on} + -0.00107629 * \text{E} - \text{angle}\hat{} \quad (2)$$

Residual analysis has been used to assess the adequacy of the constructed regression model of (MH). Figures 11 and 12 illustrate the graphical representation of the relationship between externally studentized residuals and normal probability and the actual vs. predicted values of MH, respectively. The plot results suggest a linear relationship between the actual MH values and predicted MH values, indicating a strong agreement between the two sets of data. Therefore, the proposed MH approach has considerable significance.

Table 8: MH ANOVA

Source	Sum of Squares	df	Mean Square	F-value	p-value	
Model	93.98	6	15.66	14.79	< 0.0001	significant
A-E-angle	7.19	1	7.19	6.79	0.0158	
B-Current	52.91	1	52.91	49.95	< 0.0001	
C-Pulse-on	10.86	1	10.86	10.25	0.0040	
D-Pulse-off	7.23	1	7.23	6.82	0.0156	
BC	7.23	1	7.23	6.83	0.0155	
A^2	8.55	1	8.55	8.07	0.0093	
Residual	24.36	23	1.06			
Lack of Fit	19.62	18	1.09	1.15	0.4802	not significant
Pure Error	4.75	5	0.9490			
Cor Total	118.34	29				
Std. Dev.	1.03					
Mean	21.49					
C.V. %	4.79					
R^2	0.7941					
Adjusted R^2	0.7404					
Predicted R^2	0.5244					
Adeq Precision	13.3878					

Response surface methodology creates three-dimensional (3D) Contour diagrams for the MH model in Design Expert 12 (DX 12). The correlation of the input variables and the micro-hardness can be better understood with 3D response Contour diagrams. Figure 13a shows a three-dimensional (3D) Contour diagram of an RSM model showing the impacts of electrode angle with Pulse-on and peak current on micro-hardness while keeping a constant amount of Poff = 110µs. It has been determined that there is a continuous increase in maximum MH with an electrode angle of 67.5o. There has been a rise in the magnitude of the highest current. It was noticed according to the variance of max MH, with peak current and pulse on. This increase in maximum MH at the highest current and pulse results from better-expelling power in the parking area, making melting and vaporizing the work material easier.

A significant quantity of thermal energy resulting from a max current can cause the breakdown of both the tool and the work material, ultimately leading to the melting of the work surface. The impact of the electrode angle fixed at (0º), along with the pulse on time (Pon) and peak current, on the minimal MH is illustrated in Figure 13b using a three-dimensional Contour diagram. The level of Poff remains at a constant value of 80 µs. The phenomenon of minimum (MH) shows variability in both the pulse on time and peak current, which variations in the electrical and physical characteristics of the copper electrode can explain.

Additionally, while maintaining the amount of Pon =300µs constant, Figure 13c illustrates the impact of electrode angle with pulse off (µs) and peak current on maximum MH. The correlation between the maximum microhardness (MH) at an angle of 67.5º and the current has been examined, leading to the inference that a rise in peak current at the maximum value with the pulse off results in an essential rise in microhardness. The enhancement in mental health is observed with the increase in pulse amplitude and current, which can be attributed to the prolonged pulse period. Consequently, the long-term presence of heat energy within the machining area leads to an enhancement in microhardness.

Figure 13d illustrates that the minimum MH decreases continuously when the peak current decreases to its minimum value with minimum pulse-off. Due to the low heating temperature for the shorter duration, MH decreases as pulse off time and peak current decrease. Hence, lower levels of Ip and Pon with a 22.5º electrode angle should be avoided to reduce hardness.

Figure 14a displays the maximum MH's response to varying the electrode angle from 67.5 degrees with Poff and Pon, yet keeping a constant current of 30 Amp, after observing the relationship between MH and pulse at maximum value with a relatively large current, it is determined that MH constantly increased at maximum value. Even while the peak current was rising, MH performance was getting better.

A significant quantity of thermal energy supplied for a prolonged time in the machining region is responsible for the increased MH that occurs with an increase in the pulse-off.

Similarly, the effects of electrode angle 22.5º with pulse off (µs) and pulse on time (µs) on Micro hardness, maintaining the level of Ip = 20 Ampere constant, is shown in Figure 14b. The microhardness varies with pulse on and pulse off at minimum value at lower pulse on and pulse off with minimum current (20 A).

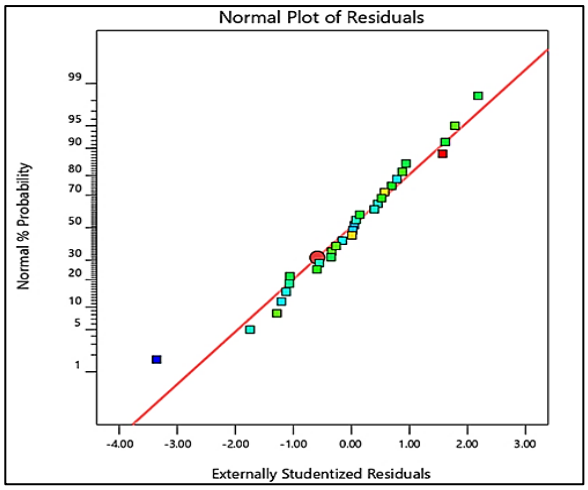

Figure 11: Normal vs. Externally studentized residuals

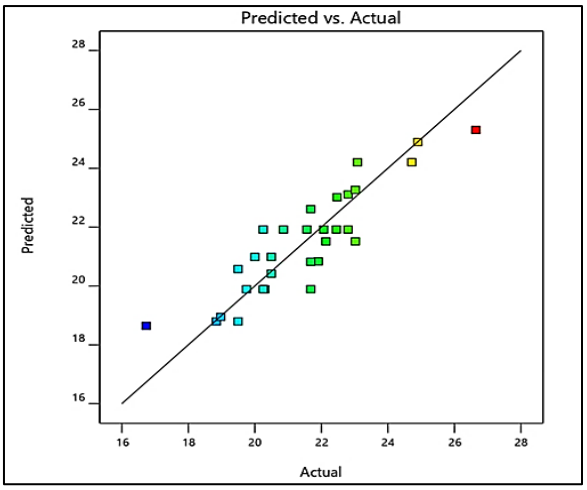

Figure 12: Predicted vs. Actual SR

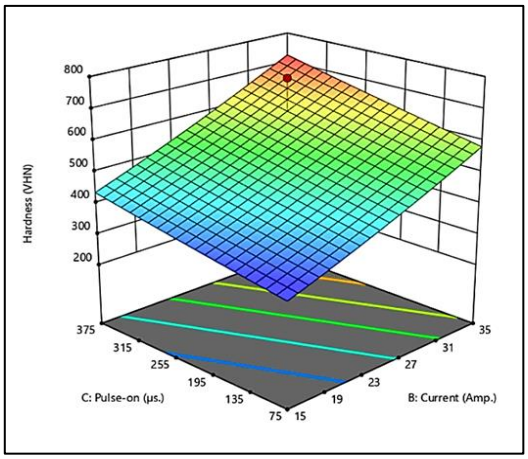

(a)

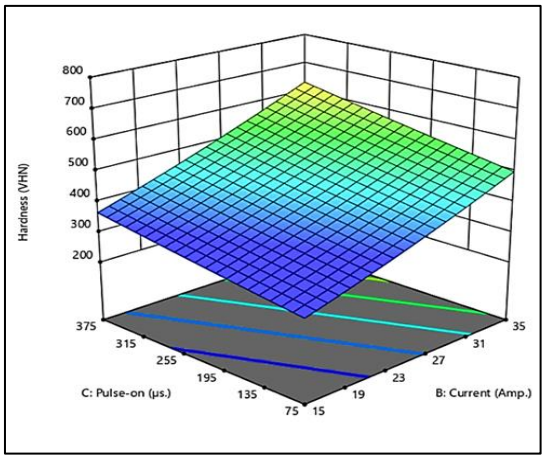

(b)

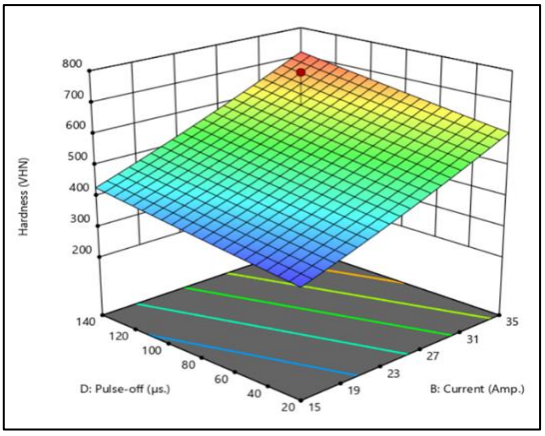

(c)

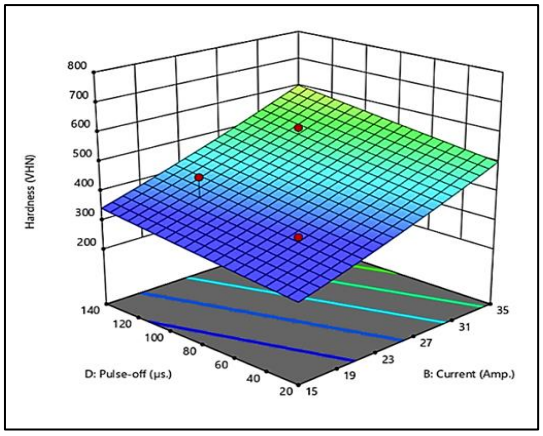

(d)

Figure 13: (a) Max MH vs. P_{on} and Current, (b) Min MH vs. P_{on} and current, (c) Max MH vs. P_{off} and current, (d) Min MH vs. P_{off} and current

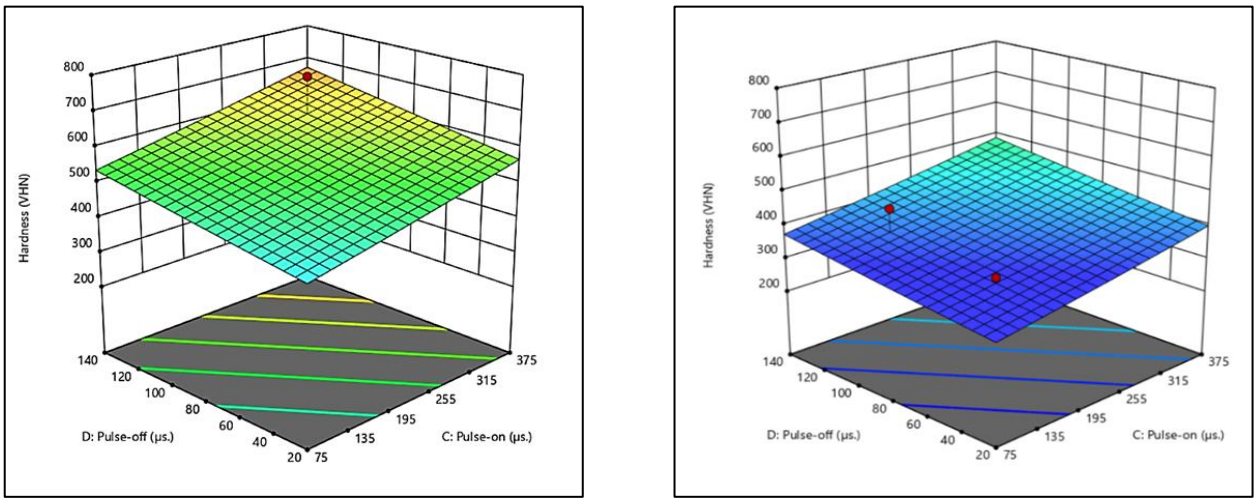

(a) **(b)**

Figure 14: (a)Max MH vs. P_{off} and $P_{on,}$ (b) Min MH vs. P_{on} and P_{off}

5. Conclusions and Recommendations

In the present experimental work, the productivity accuracy of Alloy tool steel X210 components using copper electrodes in the form of different electrode angles with transverse holes has been investigated for the EDM process. The effect of different parameters such as electrode angle (EA), peak current (Ip), pulse on time (Pon), and pulse off time (Poff) have been investigated using response surface methodology (RSM). Experimental (DOE) techniques were designed for 30 runs for four parameters for five levels to investigate the effects on output results (SR and MH).

A Central Composite Design (CCD) statistics technique has been used. A complete analysis of variance (ANOVA) was done to determine the most influential parameters. Responses (SR and MH) were modeled using RSM. The experiment obtained the lowest SR reading of 3.44133 µm when conducted with an electrode tilt of 45º, a peak current of 15 A, a pulse on-time of 225 µs, and a pulse of time of 80º µs.

Experiments were conducted using a reduced peak current value as the primary contributing factor in achieving a desirable surface finish. At an electrode inclination of 67.5º, with a maximum current of 30 amperes, a pulse on duration of 300 µs, and a pulse off time of 110 µs, the highest value of MH recorded is 720 VH. High microhardness at an electrode inclination of 67.5º is achieved by increasing the peak current and pulse duration. Dies and pressing tool durability can be significantly increased by using this approach to increase microhardness, increasing resistance to wear and abrasion. It's clear from the coefficient of variation that (C.V) values with the range that gives the model precisions with the responses. A good agreement exists between predicted and actual values for both responses, surface roughness, and hardness.

Author contributions

Conceptualization, A. Abbas. and A. Khleif; methodology; software, A. Abbas; validation, A. Abbas and A. Khleif.; formal analysis, A. Abbas; investigation, A. Abbas; resources, A. Abbas; data curation, A. Abbas; writing—original draft preparation, A. Abbas; writing—review and editing, A. Abbas; visualization, A. Abbas; supervision, A. Abbas; project administration, A. Abbas. All authors have read and agreed to the published version of the manuscript.

Funding

This research received no specific grant from any funding agency in the public, commercial, or not-for-profit sectors.

Data availability statement

The data that support the findings of this study are available on request from the corresponding author.

Conflicts of interest

The authors declare that there is no conflict of interest.

References

[1] El-Hoffy, H., Advanced Machining Processes, McGraw-Hill Company. 2005.

[2] M.M. Ali, A.F. Ibrahim, Effect of Machining Parameters on Surface Roughness and Metal Removal Rate for AISI 310 L Stainless Steel in WEDM, J. Eng. Technol., 40 (2022) 181-188. https://doi.org/10.30684/etj.v40i1.2060

[3] Jain,V.K. Advanced Machining Processes, Allied Publishers, New Delhi, India, 2004.

[4] S.A. Taqi, S.K. Shather, Investigation the Effect of Negative Polarity of Surface Roughness and Metal Removal Rate During EDM Process, J. Eng. Technol., 2020. 38(12A): p. 1852-1861. https://doi.org/10.30684/etj.v38i12A.1591

[5] Y.Q Laibi, S.K. Shather, Effect of SiC-Cu Electrode on Material Removal Rate, Tool Wear and Surface Roughness in EDM Process, J. Eng. Technol., 38 (2020) 1406-1413. https://doi.org/10.30684/etj.v38i9A.552

[6] A. Abbas, A.A. Khleif, The Influence of Angled Electrodes on Various Characteristics in EDM Process - Review Article, Tikrit. J. Eng. Sci., 30 (2023) 1-9. https://doi.org/10.25130/tjes.30.2.1

[7] S.K. Ghazi, Investigation the Electrode Wear Rate and Metal Removal Rate in EDM Process using Taguchi and ANOVA Method, J. Eng. Technol., 38 (2020) 1504-1510. https://doi.org/10.30684/etj.v38i10A.1231

[8] B. Singh, B.S. Pabla, M. Saroha, Investigating the effects of process parameters on MRR in WEDM using Molybdenum wire, Int. J. Eng. Bus. Enterpr. Appl., 9 (2014) 1-5.

[9] A.A. Khleif, O.S. Sabbar, Electrode Wear Evaluation in E.D.M Process, Eng. Technol. J., 37 (2019) 252-257. https://doi.org/10.30684/etj.37.2C.9

[10] A. A.Khan, M. Y.Ali, Md. M. Haque, A Study of Electrode Shape ConFigureuration on The Performance of Die Sinking EDM, Int. J. Mech. Mater. Eng., 4 (2009) 19-23.

[11] J. Kumar, T. Soota, S.K. Rajput, Machining of Zircaloy-2 using progressive tool design in EDM, Mater. Manuf. Processes, 37 (2022) 1746-1755. https://doi.org/10.1080/10426914.2022.2049299

[12] N. A. Mufti, M. Rafaqat, N. Ahmed, M. Q. Saleem, A. Hussain, A.M. Al-Ahamri, Improving the Performance of EDM through Relief-Angled Tool Designs, Appl. Sci., 10 (2020) 2432. https://doi.org/10.3390/app10072432

[13] N. Pellicer, J. Ciurana, T. Ozel, Influence of Process Parameters and Electrode Geometry on Feature Micro-Accuracy in Electro Discharge Machining of Tool Steel, Mater. Manuf. Processes, 24 (2009) 1282-1289. https://doi.org/10.1080/10426910903130065

[14] R. Davis, A. Singh, F.L. Amorim, M.J. Jackson, W.F. Sales, Effect of Tool Geometry on the Machining Characteristics amid SiC Powder Mixed Electric Discharge Drilling of Hybrid Metal Matrix Composite, Silicon, 14 (2020) 27-45. https://doi.org/10.1007/s12633-020-00763-0

[15] S. Pani, M. Masanta, Experimental Analysis of AA6063 Aluminium Alloy Machining by EDM with Hexagonal Shaped Tool Electrode, Mater. Today: Proc., 18 (2019) 2723-2730. https://doi.org/10.1016/j.matpr.2019.07.135

[16] M. Toche, A. Tajane, Effect of electrode geometrical parameters in die sink EDM A Review, Int. J. Adv. Res. Innov. Ideas Educ., 3 (2017) 2395-4396.

[17] J. Li, X.H. Zhou, W. Liu, H. Ma, A new approach for uncut detection and automatic design of EDM electrodes, Int. J. Adv. Manuf. Technol., 104 (2019) 599-615. https://doi.org/10.1007/s00170-019-03923-8

[18] K.V. Dave, D.S. Patel, Influence of Electrode Geometry and Process Parameters on Surface Quality and MRR in Electrical Discharge Machining (EDM) of AISI H13, Int. J. Eng. Res. Appl., 3 (2012) 1498-1505.

[19] B. Jha, K. Ram, M. Rao, An overview of technology and research in electrode design and manufacturing in sinking electrical discharge machining, J. Eng. Sci. Technol. Rev., 4 (2011) 118-130. http://dx.doi.org/10.25103/jestr.042.02

[20] S.K. Shather, A.F. Ibrahim, Z.H. Mohsein, O.H. Hassoon, Enhancement of EDM Performance by Using Copper-Silver Composite Electrode, J. Eng. Technol., 38 (2020) 1352-1358. https://doi.org/10.30684/etj.v38i9A.1549

[21] N. Asif, M.Q. Saleem, M.U. Farooq, Performance evaluation of surfactant mixed dielectric and process optimization for electrical discharge machining of titanium alloy Ti6Al4V, CIRP J. Manuf. Sci. Technol., 43 (2023) 42-56. https://doi.org/10.1016/j.cirpj.2023.02.007

[22] S.A. Khan, M. Rehman, M.U .Farooq, M.A. Ali, R. Naveed, A Detailed Machinability Assessment of DC53 Steel for Die and Mold Industry through Wire Electric Discharge Machining, Metals,11 (2021) 816. https://doi.org/10.3390/met11050816

[23] M.B. Ndaliman, A.A. Khan, M.Y. Ali, Influence of electrical discharge machining process parameters on surface micro-hardness of titanium alloy, Proc. Inst. Mech. Eng., Part B: J. Eng. Manuf., 227 (2013) 460-464. http://dx.doi.org/10.1177/0954405412470443